universität
uulm

Faculty of Natural Sciences
Institute of Quantum Physics

Bachelor Thesis at Ulm University

What can we learn from the Phase of the Momentum Wave Function?

Submitted by
André Knoll
andre.knoll@uni-ulm.de

Supervisor
Prof. Dr. Wolfgang P. Schleich

2025

Abstract

Due to the Born rule of quantum mechanics, the amplitude of the wave function is often emphasized, while the phase is frequently overlooked. However, a closer examination reveals that the phase, particularly when encoded by the Fourier transform of position space, contains critical information about the original wave function. Building on signal processing techniques introduced by Oppenheim et al. in 1981 (Proc. IEEE, 69, 5, pp. 529 - 541), we adapt and extend these methods to the quantum mechanical framework. In particular, we show that even when we replace the amplitude of the momentum wave function by a constant, the phase of the momentum wave function allows a partial reconstruction of the position wave function. Our findings underscore the fundamental role of the phase in Fourier-based transformations, offering new insights into quantum mechanics and potential applications in quantum information science.

Contents

1 Introduction **4**

2 The Oppenheim-Lim-Protocol **6**
2.1 The original Protocol 6
2.2 Translation into Quantum Mechanics 7

3 Reconstruction of an exemplary Wave Function **10**
3.1 The momentum Wave Function and its Phase 10
3.2 Numerical Reconstruction the Wave Function 15
3.3 Approximation via Legendre Series Expansion 18
3.3.1 Lowest order Approximation 24

4 Discussion and Conclusion **28**

Bibliography **30**

A Appendix **32**
A.1 The protocol applied to a single Gaussian 32
A.2 The Wigner Function of the exemplary Wave Function 33
A.2.1 The Interference term 36
A.3 Relative Difference between the Legendre and Numerical Reconstruction 38

1 Introduction

The amplitude of wave functions in quantum mechanics has traditionally been the primary focus, as according to the Born rule, it is directly related to the probability densities of the state [1]. In contrast, the phase of the wave function often receives less attention, despite its crucial role in phenomena such as interference and coherence. A deeper understanding of the phase, in particular the phase of the momentum wave function, could provide new insights into quantum mechanics and its applications.

To be precise, the goal of this thesis is to reconstruct the position wave function from the phase of the momentum wave function. With a focus on phase-only reconstruction, the aim is to uncover wether the phase alone is enough to partially recover the integral parameters of a quantum state.

The Fourier transform serves as the main tool in this endeavour, as it enables transformation between the momentum and position space representations of wave functions [2]. Inspired by the work of Oppenheim and Lim [3, 4], who demonstrated the crucial role of the phase in signal processing, and its ability to allow phase based image reconstruction. By transforming an image into Fourier space and then separating phase and amplitude, they were able to show that, by applying an inverse transform onto the phase, the image could be reconstructed. The objective therefore becomes to adapt their methods for quantum mechanics.

This work attempts to demonstrate that the phase of the momentum wave function contains enough information to enable a partial reconstruction of the position wave function. The intentions are to adapt the Oppenheim-Lim protocol for application in quantum mechanical systems and to determine the effectiveness of phase-only reconstructions.

The methodology employed in this thesis involves the application of Fourier transforms to obtain momentum-space representations of wave functions, followed by the isolation of phase information. Numerical reconstruction techniques and analytical approximations, to be precise the Legendre series expansion, are utilized to validate the effectiveness of phase-only reconstruction approaches.

By translating the protocol presented by Oppenheim and Lim into quantum mechanics and demonstrating its validity, we aim to establish a foundation for utilizing the properties of Fourier-based transformations within the broader field of quantum mechanics.

In chapter 2 the protocol used by Oppenheim and Lim is discussed, and a methodology is constructed from it to apply to a wave function. Afterwards, in chapter 3 the translated

protocol is applied to an exemplary wave function, consisting of a superposition of two Gaussians, to demonstrate its validity for the given example. Finally, the protocol is reviewed in chapter 4, based on a comparisons between the original wave function and its reconstruction in previous chapters.

2 The Oppenheim-Lim-Protocol

2.1 The original Protocol

The goal of this thesis is to demonstrate the validity of the protocol used by Oppenheim et al. [3] in the realm of quantum mechanics, as a reliable way to partially reconstruct wave functions from phase information might be of future use. In order to analyze the protocol in context of quantum mechanics, it is necessary to translate it onto the framework, as in its current form, it is to be applied onto images. Thus our first step becomes to summarize their method. The group demonstrated how the decomposition of an image into its Fourier components can reveal the distinct roles of the phase and amplitude in reconstructing the image [5]. Their approach highlights the significance of the phase in retaining structural information. The steps of their protocol are as follows [3]:

1. Start with a regular image and transform it into the frequency domain using a Fast Fourier Transform (FFT). This conversion decomposes the image into its Fourier domain representation.
2. Separate the phase term from the amplitude. This step allows for independent analysis of these components and their respective contributions to the image reconstruction.
3. Perform the following reconstructions by applying an inverse Fast Fourier Transform (IFFT) to combinations of the phase and amplitude:
    a) Use the phase term combined with a constant amplitude. By setting the constant equal to, either one or the average amplitude, as the later produces a closer reconstruction. The resulting image retains only the structural outlines of the original.
    b) Use only the amplitude without the phase. The reconstructed image is nearly entirely black, demonstrating the minimal contribution of the amplitude to the visual structure.

While the FFT is an approximation of a discrete Fourier transform optimized for digital computation, which uses the symmetries present within the DFT to decrease the necessary computation. By making a few assumptions on the behavior of the signal, for example a perfect sampling, the FFT still provides an almost exact result. The DFT is the discrete variant of the regular Fourier transform, which calculates the transforma-

tion via a sum of samples gathered from the original signal. The DFT is mathematically equivalent to the Fourier transform for a finite signal [6].

The results from this protocol, including the three distinct reconstructions, demonstrate the pivotal role of the phase in preserving structural information of the original signal. Similar reconstructions, except for the reconstruction created using only the amplitude, are shown in fig. 2.1.

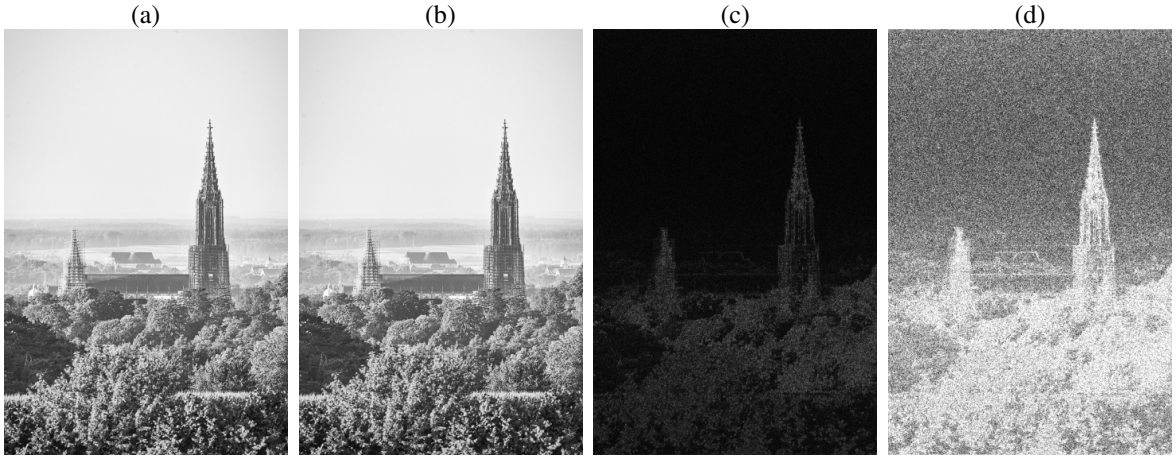

Figure 2.1: Reconstructions of the image performed using a method similar to that used by Oppenheim et al. [3]. **(a)** shows the original picture of the Ulm Minster. **(b)** is the result of applying a FFT and IFFT to the image, demonstrating the reconstructive properties of these transformations. **(c)** is a reconstruction using only the phase term with an unitary amplitude; the image was brightened by a factor of 15 for better visibility. **(d)** is a reconstruction based on the phase term multiplied by the average amplitude; this image was also brightened by the same factor. In comparison, the last two images differ mainly in their contrast: the third picture is relatively dark, while the fourth is much brighter and more detailed.

These results indicate that, for an arbitrary signal, at least some of the original structure can be reconstructed from the phase of its Fourier transform alone. Furthermore, the amplitude, when averaged, provides a scaling factor that brings the reconstruction closer to the original image.

2.2 Translation into Quantum Mechanics

In order to apply the above discussed protocol onto a wave function, it is necessary to translate it into a quantum mechanical framework. The protocol is based upon Fourier transforms, which are common place in quantum mechanics, as they are used tor transform between position and momentum space representations of the wave function [7].

The first step is therefore to replace the signal with a one dimensional wave function $\psi(x)$, which describes an initial state in position space. The wave function $\psi(x)$ is normalized and square integrable, satisfying the condition

$$\int_{-\infty}^{\infty} \mathrm{d}x \, |\psi(x)|^2 = 1. \tag{2.1}$$

Despite this condition, our focus lies primarily on the wave function itself rather than its absolute value during the reconstruction process.

To proceed, translating the protocol into mathematical operations becomes necessary. The first step of the original protocol was to apply a FFT to the signal. Instead a regular Fourier transform is utilized as our goal is to obtain a non numerical solution.

The aim now becomes to Fourier transform the wave function into momentum space via

$$\Phi(p) \equiv \frac{1}{\sqrt{2\pi}} \int_{-\infty}^{\infty} \mathrm{d}x \, e^{\frac{\mathrm{i}}{\hbar}px} \, \psi(x). \tag{2.2}$$

Thus the momentum wave function $\Phi(p)$ is obtained by performing the Fourier integral in eq. (2.2). After obtaining the Fourier space representation of the signal, the protocol proceeds by separating the amplitude and phase of the signal. By utilizing the definition of the complex number

$$\Phi(p) = |\Phi(p)|e^{\mathrm{i}\varphi} \tag{2.3}$$

and then rearranging, an expression for the phase term is obtained. In the protocol the resulting signal is transformed back into image space. To accomplish this, the inverse Fourier transform is used. The previously obtained phase term can thus be substituted into the inverse Fourier integral

$$\tilde{\psi}(x) \equiv \frac{1}{\sqrt{2\pi}} \int_{-\infty}^{\infty} \mathrm{d}p \, e^{-\frac{\mathrm{i}}{\hbar}px} \, \frac{\Phi(p)}{|\Phi(p)|} \tag{2.4}$$

$$\psi(x) = \frac{1}{\sqrt{2\pi}} \int_{-\infty}^{\infty} \mathrm{d}p \, e^{-\frac{\mathrm{i}}{\hbar}px} \, \Phi(p), \tag{2.5}$$

to calculate the reconstructed function $\tilde{\psi}(x)$. Some differences between the original wave function $\psi(x)$, eq. (2.5), and its reconstruction $\tilde{\psi}(x)$, eq. (2.4), are already clear, as the integrand of the two functions differ by a factor $1/|\Phi(p)|$. In the case where the absolute value $|\Phi(p)|$ is constant, the integrals are equivalent up to said constant. If the absolute value is momentum dependent, it is not obvious that there are similarities between $\psi(x)$ and $\tilde{\psi}(x)$. In order to demonstrate the similarities between the two functions $\psi(x)$ and $\tilde{\psi}(x)$, they will be compared by analyzing their respective graphs.

In order to show the plausibility of the reconstruction process, a exemplary wave function

will be reconstructed using the protocol.

With the protocol established, it can be summarized concisely as a three-step process applied to a given wave function $\psi(x)$:

1. Calculate the momentum space representation $\Phi(p)$ via a Fourier transform.
2. Determine the phase factor via $\frac{\Phi(p)}{|\Phi(p)|}$.
3. Reconstruct the wave function $\tilde{\psi}(x)$ using an inverse Fourier transform.

This protocol allows for phase-only reconstructions of the wave function, either with a unitary amplitude or an average amplitude, as the latter is a scalar factor applied to the reconstructed wave function afterwards. A diagram showing this process can be seen in fig. 2.2.

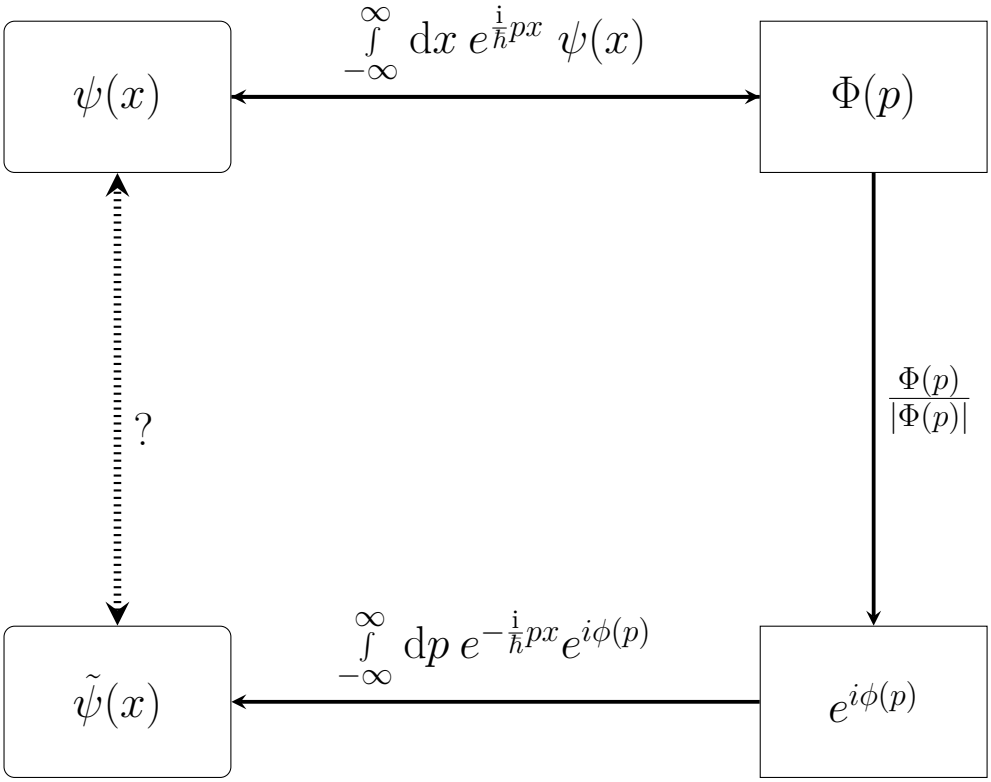

Figure 2.2: Flowchart detailing the protocol [3] discussed in section 2.2, it contains the following steps: **(1)** compute the Fourier transform, **(2)** calculate the phase by dividing the function by its absolute value,**(3)** apply an inverse Fourier transform, and finally compare the reconstruction with the original function.

3 Reconstruction of an exemplary Wave Function

3.1 The momentum Wave Function and its Phase

With the protocol now well defined for an application in quantum mechanics, the aim now becomes to demonstrate it's validity, by applying it to an example wave function. The goal of this section is to demonstrate the previously suspected similarities between the reconstruction $\tilde{\psi}(x)$ and the original $\psi(x)$ by applying the protocol on to example a wave function. By comparing the reconstruction with the original, once the protocol is completed, the similarities and differences between them will become visible. The wave function being utilized is a superposition of two Gaussians, both located at a set distance x_0 symmetrically around the origin. This function was chosen, as the Gaussian is a common state within quantum mechanics. The main difference, besides their location, is their respective widths, given by σ_1 and σ_2. For this section all plots are created with the following values, $\sigma_1 = 2$, $\sigma_2 = 0.1$, $x_0 = 5$ and finally $\hbar = 1$. Thus the starting wave function is given by

$$\psi(x) \equiv \frac{1}{N}\left(\frac{1}{\sqrt[4]{\pi\sigma_1^2}} e^{-\frac{1}{2}\frac{(x-x_0)^2}{\sigma_1^2}} + \frac{1}{\sqrt[4]{\pi\sigma_2^2}} e^{-\frac{1}{2}\frac{(x+x_0)^2}{\sigma_2^2}}\right), \tag{3.1}$$

with a normalization constant N, which can be obtained by normalization via (2.1). Due to the wave function in eq. (3.1) being a linear combination of regular Gaussians, it is possible to rewrite the expression as

$$\psi(x) = \frac{1}{N}\psi_1(x - x_0) + \frac{1}{N}\psi_2(x + x_0), \tag{3.2}$$

with $\psi_{\mathrm{n}}(x) = \frac{1}{\sqrt[4]{\pi\sigma_{\mathrm{n}}^2}}\, e^{-\frac{1}{2}\frac{x^2}{\sigma_{\mathrm{n}}^2}}$. Following the protocol presented before, the Fourier transform has be applied to the wave function $\psi(x)$, in order to determine it's momentum space representation $\Phi(p)$. Due to the linearity of the transform, the integral decomposes into the two transforms for $\psi_{\mathrm{n}}(x)$ individually and afterwards has to be recombined to obtain the transformed wave function. Transforming a single Gaussian ψ_{n}, using the

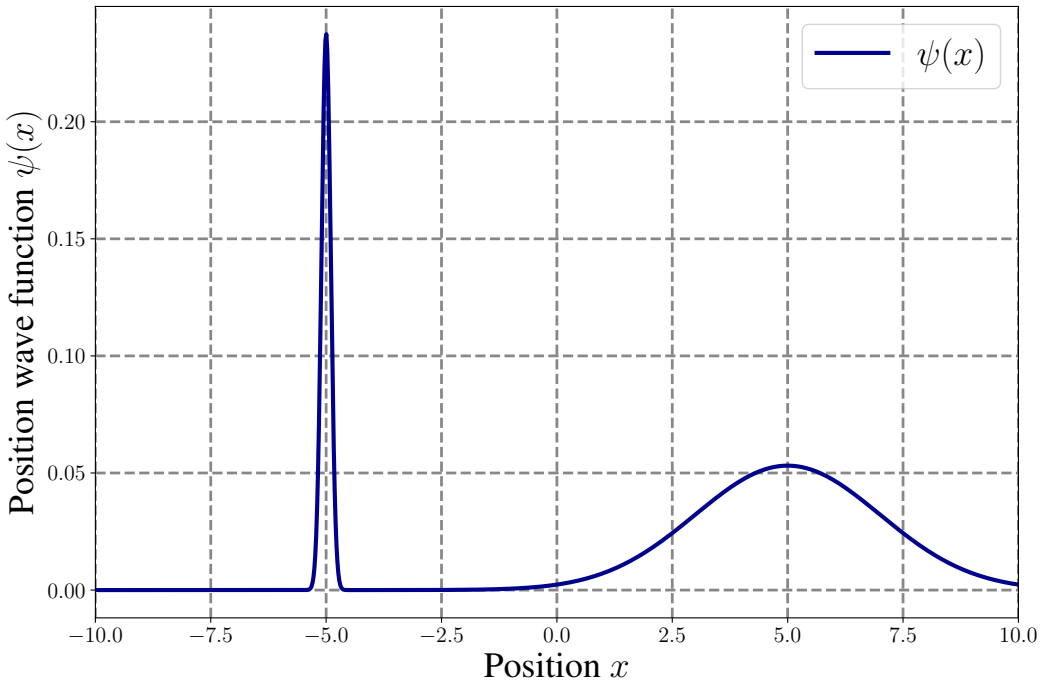

Figure 3.1: Plot of the original wave function $\psi(x)$ in position space given by (3.1). There are two distinct Gaussian peaks located at x_0 and $-x_0$. No interference is visible in between the two peaks.

Fourier integral,

$$\Phi_{\mathrm{n}}(p) \equiv \frac{1}{\sqrt{2\pi}} \int_{-\infty}^{\infty} \mathrm{d}x \, e^{\frac{\mathrm{i}}{\hbar} px} \psi_{\mathrm{n}}(x), \tag{3.3}$$

provides the necessary momentum space representation $\Phi_n(p)$ of a single Gaussian. This integration can be done using the formula for Gaussian integrals [2], where

$$\Phi_{\mathrm{n}}(p) = \sqrt[4]{\frac{\sigma_{\mathrm{n}}^2}{\pi}} e^{-\frac{1}{2}\frac{p^2}{\hbar^2}\sigma_{\mathrm{n}}^2}. \tag{3.4}$$

is also a Gaussian, due to the property of Gaussian functions, remaining Gaussians after applying a Fourier transform. By using another property of the Fourier transform [2], that any displacement of the original function becomes a phase for the transformed term, the displacement of the original Gaussian can be included via

$$\mathcal{F}[\psi(x - x_0)] = \mathcal{F}[\psi(x)] \, e^{-\frac{\mathrm{i}}{\hbar} p x_0}. \tag{3.5}$$

After the transform is performed and the two Gaussians are obtained, each is multiplied

with its respective phase, resulting in the momentum space wave function

$$\begin{aligned}\Phi(p) &\equiv \frac{1}{N}\left[\Phi_1(p)\, e^{-\frac{\mathrm{i}}{\hbar}px_0} + \Phi_2(p)\, e^{-\frac{\mathrm{i}}{\hbar}px_0}\right] \\ &= \frac{1}{N}\left(\sqrt[4]{\frac{\sigma_1^2}{\pi}} e^{-\frac{1}{2}\frac{p^2}{\hbar^2}\sigma_1^2 - \frac{\mathrm{i}}{\hbar}px_0} + \sqrt[4]{\frac{\sigma_2^2}{\pi}} e^{-\frac{1}{2}\frac{p^2}{\hbar^2}\sigma_2^2 + \frac{\mathrm{i}}{\hbar}px_0}\right),\end{aligned} \tag{3.6}$$

which still contains two Gaussians, due to the chosen position wave function $\psi(x)$ and remains normalized. A depiction of the relative behavior of the two Gaussians can be seen in fig. 3.2

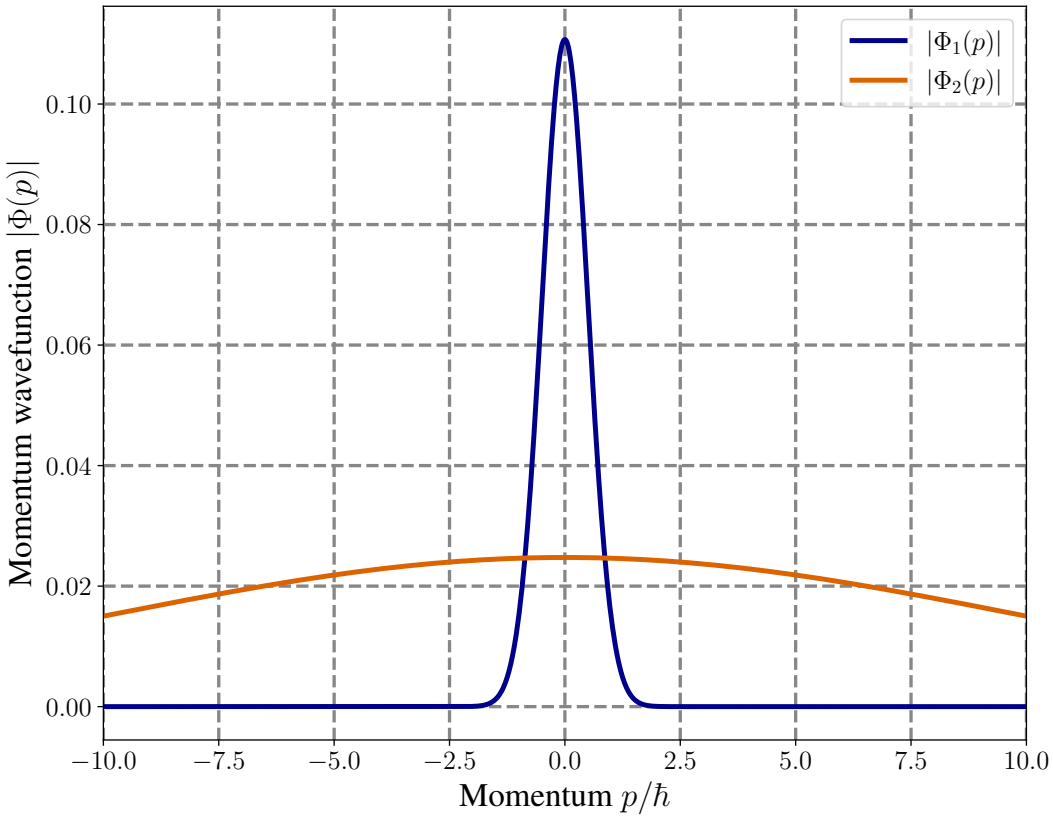

Figure 3.2: Plot of the absolute value of two terms of the momentum wave function $|\Phi_1(p)|$ and $|\Phi_2(p)|$, as seen in eq. (3.4). The two different Plots show the behavior of the absolute value of each of the two Gaussians, which in sum make up the momentum wave function.

In order to stay by the protocol discussed in section 2.2, it now becomes necessary to calculate the phase term of the momentum wave function. This can be achieved by

calculating the absolute value $|\Phi(p)|$. In order to simplify notation

$$R_n = \sqrt{\sigma_n} e^{-\frac{1}{2}\frac{p^2}{\hbar^2}\sigma_n^2} \tag{3.7}$$

is introduced and the function is split into its real and imaginary part:

$$\Phi(p) = \frac{1}{N\sqrt[4]{\pi}}\left[(R_1 + R_2)\cos\left(\frac{px_0}{\hbar}\right) + \mathrm{i}(R_2 - R_1)\sin\left(\frac{px_0}{\hbar}\right)\right] \tag{3.8}$$

After utilizing the general formula to calculate the absolute value for any given complex number $|\Phi(p)| = \sqrt{\mathrm{Re}\{\Phi(p)\}^2 + \mathrm{Im}\{\Phi(p)\}^2}$, and inserting the real and imaginary parts, as found in eq. (3.8),

$$|\Phi(p)| = \frac{1}{N\sqrt[4]{\pi}}\sqrt{(R_1 + R_2)^2\cos^2\left(\frac{px_0}{\hbar}\right) + (R_2 - R_1)^2\sin^2\left(\frac{px_0}{\hbar}\right)}, \tag{3.9}$$

is obtained. By expanding the brackets and afterwards utilizing an addition theorem for sine and cosine, namely $\cos^2(x) - \sin^2(x) = \cos(2x)$, the expression for the absolute value simplifies to

$$|\Phi(p)| = \frac{1}{N\sqrt[4]{\pi}}\sqrt{R_1^2 + R_2^2 + 2R_1R_2\cos\left(2\frac{px_0}{\hbar}\right)}. \tag{3.10}$$

The general behavior of a function of this form can be seen in fig. 3.3. After calculating the absolute value, it is possible to determine the phase term by utilizing eq. (2.3). This results in the following expression

$$e^{\mathrm{i}\varphi(p)} = \frac{\Phi(p)}{|\Phi(p)|} = \frac{R_1 e^{-\frac{\mathrm{i}}{\hbar}px_0} + R_2 e^{\frac{\mathrm{i}}{\hbar}px_0}}{\sqrt{R_1^2 + R_2^2 + 2R_1R_2\cos\left(2\frac{px_0}{\hbar}\right)}}. \tag{3.11}$$

In order to proceed with the protocol, the next step is to apply an inverse Fourier transform on the phase term, in order to get an expression for the reconstructed wave function $\tilde{\psi}(x)$. This can be done by plugging the phase term into the corresponding Fourier integral and integrating the expression. Thus, an integral form, for the reconstructed wave function, is obtained

$$\tilde{\psi}(x) \sim \int_{-\infty}^{\infty} \mathrm{d}p e^{-\frac{\mathrm{i}}{\hbar}px}\frac{\Phi(p)}{|\Phi(p)|} = \int_{-\infty}^{\infty} \mathrm{d}p e^{-\frac{\mathrm{i}}{\hbar}px}\frac{R_1 e^{-\frac{\mathrm{i}}{\hbar}px_0} + R_2 e^{\frac{\mathrm{i}}{\hbar}px_0}}{\sqrt{R_1^2 + R_2^2 + 2R_1R_2\cos\left(2\frac{px_0}{\hbar}\right)}}. \tag{3.12}$$

This is the integral expression for the reconstructed wave function $\tilde{\psi}(x)$, which enables a numerical integration, as due to the nonlinear denominator an analytical solution, at least without approximation, is not feasible.

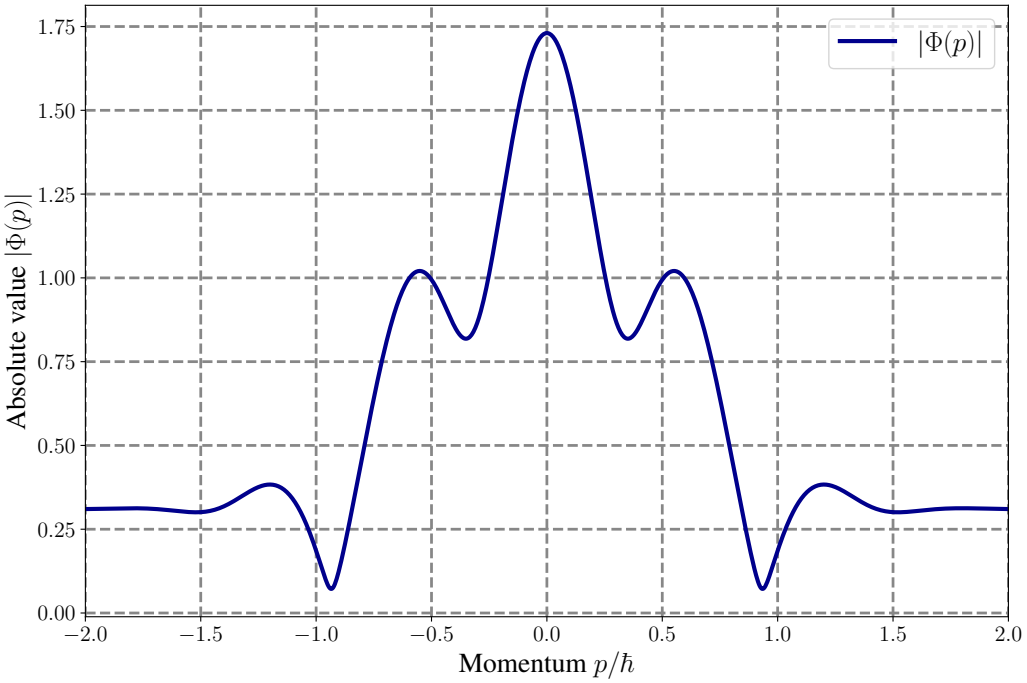

Figure 3.3: Plot of the formula for the absolute value $|\Phi(p)|$ as seen in eq. (3.10). The function is plotted without the normalization constant, as only its general behavior is of interest rather than its amplitude. The function shows Gaussian like behavior, but is disturbed by the cosine term, which rather quickly decreases.

3.2 Numerical Reconstruction the Wave Function

In order to proceed, the integral form of $\tilde{\psi}(x)$, as seen in eq. (3.12), was solved numerically. This due to the denominator involving nonlinear terms that mix exponential and oscillatory behavior, which prevent simplification. As well as the numerator and denominator are coupled preventing factorization or a separation into simpler integrals.

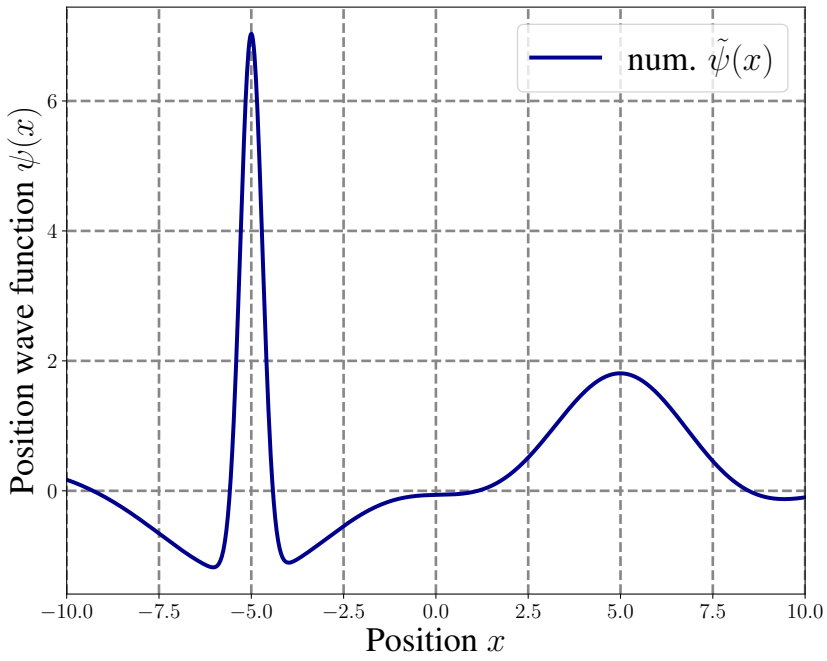

Figure 3.4: Numerical integration of the integral representation of the reconstructed position wave function $\tilde{\psi}(x)$ shown in eq. (3.12). The integration was performed by using the SciPy [8] library.

When comparing the reconstructed wave function $\tilde{\psi}(x)$, depicted in fig. 3.4, to the original function $\psi(x)$, as seen in fig. 3.1, a few key differences emerge. For one in contrast to the original wave function $\psi(x)$ the numerical reconstruction of the wave function $\tilde{\psi}(x)$ is not normalized. This is expected due to the nature of protocol. It is also apparent that oscillations occur with in the reconstructed wave function, causing among others the valley around the first peak at $x = -5$. This disturbance can be seen more clearly in fig. 3.5, where the reconstruction does not drop to zero, in comparison to a regular Gaussian, but rather oscillates with decreasing amplitude. These oscillations occur due to the cosine term present within the denominator.

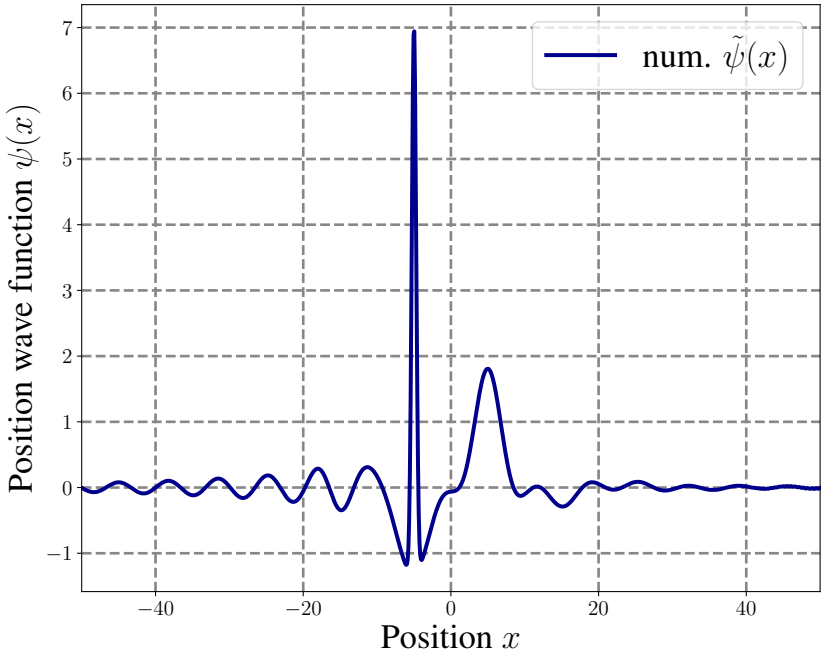

Figure 3.5: Numerical integration of the reconstructed position wave function $\tilde{\psi}(x)$ shown in eq. (3.12). The integration was performed by using the SciPy library [8]. Here the values from -50 to 50 are plotted, in order to more clearly show the oscillations affecting the reconstruction.

Another difference that is worth pointing out lies within the widths of the peaks, as the two Gaussian peaks appear to have the same expectation value but exhibit different variances, as can be seen in fig. 3.6. It seems plausible that the protocol preserves the position exactly; however, instead of conserving the variance, it only retains a relative factor made up by the two variances. Due to the inherent complexity of the integral in eq. (3.12), it seems necessary to approximate the phase rather, than trying to compute the integration explicitly. As the absolute value $|\Phi(p)|$, as seen in eq. (3.10), is similar to the generating function of the Legendre series, the aim becomes to approximate the absolute value via a series expansion.

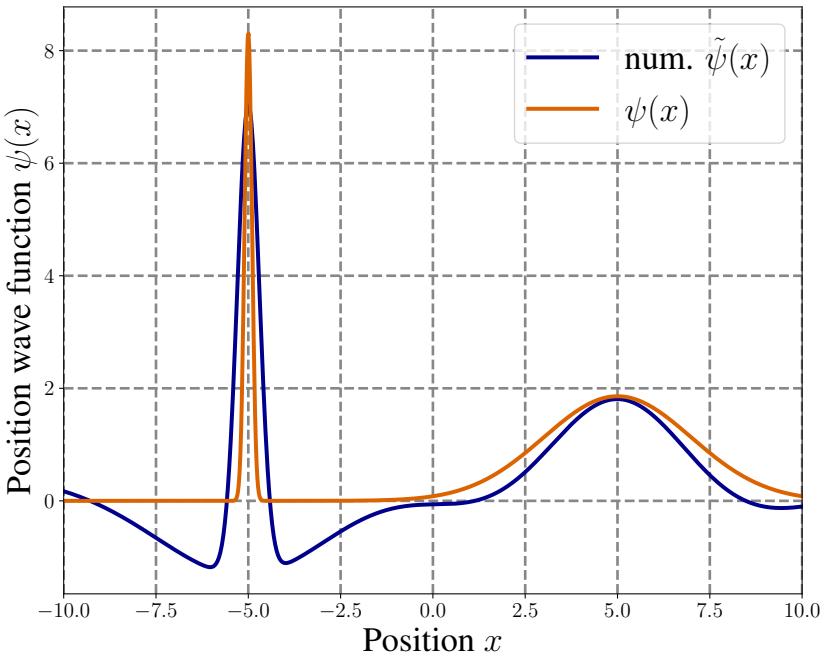

Figure 3.6: The plot depicts a comparison of the reconstructed wave function $\tilde{\psi}(x)$ to a scaled version of the original $\psi(x)$ eq. (3.1), it was scaled by the mean value of the quotient of the peaks. A very noticeable difference, besides the oscillations apparent in the reconstruction, is the difference in widths.

3.3 Approximation via Legendre Series Expansion

As the reconstruction integral $\tilde{\psi}(x)$, seen in eq. (3.12), could not be computed analytically, it seems sensible for the function to be approximated in order to circumvent this problem. By looking closer at the expression for the reciprocal of the absolute value, $1/|\Phi|$, it becomes apparent that it closely resembles the generating function for the Legendre polynomials, as seen in eq. (3.13) [9]. We can exploit this similarity to expand the reciprocal value into a series of Legendre polynomials. Such an expansion may enable for an analytic evaluation of the integral eq. (3.12) that is relatively precise even if only a few orders are taken into account. Ideally, if the lowest order alone provides a close approximation, an analytic expression might be discovered. In order to derive a Legendre series expansion of $1/|\Phi(p)|$ it becomes necessary to express the absolute value in terms of the Legendre polynomials.

The general form for the generating function of the Legendre polynomials is given by [9]

$$\frac{1}{\sqrt{r^2 + R^2 - 2rR\cos(\gamma)}} = \sum_{m=0}^{\infty} \frac{r^m}{R^{m+1}} P_m(\cos\gamma). \tag{3.13}$$

The key difference between eq. (3.10) and eq. (3.13) is the negative sign in front of the cross term. To resolve this, R_1 is set to $R_1 \to -R_1$. After applying this change, the reciprocal absolute value becomes

$$\frac{1}{|\Phi(p)|} \sim L(p) \equiv \frac{1}{\sqrt{(-R_1)^2 + R_2^2 - 2(-R_1)R_2\cos\left(2\frac{px_0}{\hbar}\right)}}. \tag{3.14}$$

To proceed, the R_n terms are substituted into the series expansion. Care must be taken when choosing wether R_1 or R_2 becomes the denominator and which term becomes the numerator, as the condition $R_< < R_>$ must hold to prevent the series $L(p)$ from diverging. By inserting the condition, it results in

$$L(p) = \sum_{m=0}^{\infty} \frac{R_<^m}{R_>^{m+1}} P_m\left(\cos\left(2\frac{px_0}{\hbar}\right)\right). \tag{3.15}$$

This requires splitting the interval into three, with the bounds corresponding to the intersection points of the two Gaussians in fig. 3.2, resulting in the following piecewise

definition:

$$\frac{R_<^m}{R_>^{m+1}} = \begin{cases} (-R_1)^m / R_2^{m+1}, & p \leq -\hbar\varepsilon \\ R_2^m / (-R_1)^{m+1}, & -\hbar\varepsilon < p < \hbar\varepsilon \\ (-R_1)^m / R_2^{m+1}, & p \geq \hbar\varepsilon \end{cases}$$

with $\varepsilon = \sqrt{\frac{\ln(\sigma_1) - \ln(\sigma_2)}{\sigma_1^2 - \sigma_2^2}}$ being the intersection points of the two Gaussians.

By inserting the series expansion into the inverse Fourier transform, the integral becomes

$$\tilde{\psi}(x) = \frac{1}{\sqrt{2\pi}} \sum_{m=0}^{\infty} \int_{-\infty}^{\infty} \mathrm{d}p \; e^{-\frac{\mathrm{i}}{\hbar}px} \; \Phi(p) \; \frac{R_<^m}{R_>^{m+1}} P_m\left(\cos\left(2\frac{px_0}{\hbar}\right)\right). \tag{3.16}$$

Using the piecewise definition, the total reconstructed wave function becomes $\tilde{\psi}(x) = I_1(x) + I_2(x) + I_3(x)$, where the three integrals are:

$$\begin{aligned} I_1(x) =& \frac{(-1)^m}{\sqrt{2\pi}} \sum_{m=0}^{\infty} \int_{-\infty}^{-\hbar\varepsilon} \mathrm{d}p \; e^{-\frac{\mathrm{i}}{\hbar}px} \; \Phi(p) \; \frac{R_1^m}{R_2^{m+1}} \; P_m\left(\cos\left(2\frac{px_0}{\hbar}\right)\right) \\ I_2(x) =& \frac{(-1)^{m+1}}{\sqrt{2\pi}} \sum_{m=0}^{\infty} \int_{-\hbar\varepsilon}^{\hbar\varepsilon} \mathrm{d}p \; e^{-\frac{\mathrm{i}}{\hbar}px} \; \Phi(p) \; \frac{R_2^m}{R_1^{m+1}} \; P_m\left(\cos\left(2\frac{px_0}{\hbar}\right)\right) \\ I_3(x) =& \frac{(-1)^m}{\sqrt{2\pi}} \sum_{m=0}^{\infty} \int_{\hbar\varepsilon}^{\infty} \mathrm{d}p \; e^{-\frac{\mathrm{i}}{\hbar}px} \; \Phi(p) \; \frac{R_1^m}{R_2^{m+1}} \; P_m\left(\cos\left(2\frac{px_0}{\hbar}\right)\right) \end{aligned} \tag{3.17}$$

with R_n as defined in eq. (3.7)

The complexity of these integrals increases with higher orders due to the combination of exponential and Legendre polynomial terms. The first five polynomials are shown in table 3.1.

Table 3.1: The Legendre polynomials up to the 5th order [9].

Order	Polynomial $P_n(x)$
0	1
1	x
2	$\frac{1}{2}(3x^2 - 1)$
3	$\frac{1}{2}(5x^3 - 3x)$
4	$\frac{1}{8}(35x^4 - 30x^2 + 3)$
5	$\frac{1}{8}(63x^5 - 70x^3 + 15x)$

The integrations were performed numerically. In fig. 3.7 numerical results from $\tilde{\psi}(x)$ (depicted in fig. 3.4) are compared with the series expansion for different orders. As the

order increases, the series matches the numerical solution even more closely. In fig. 3.8 the absolute difference $|\Delta\psi(x)| = |\tilde{\psi}(x) - \tilde{\psi}_{\mathrm{n}}(x)|$ between the numerical solution and the series expansion at various orders n is shown, demonstrating that the difference diminishes as the order increases.

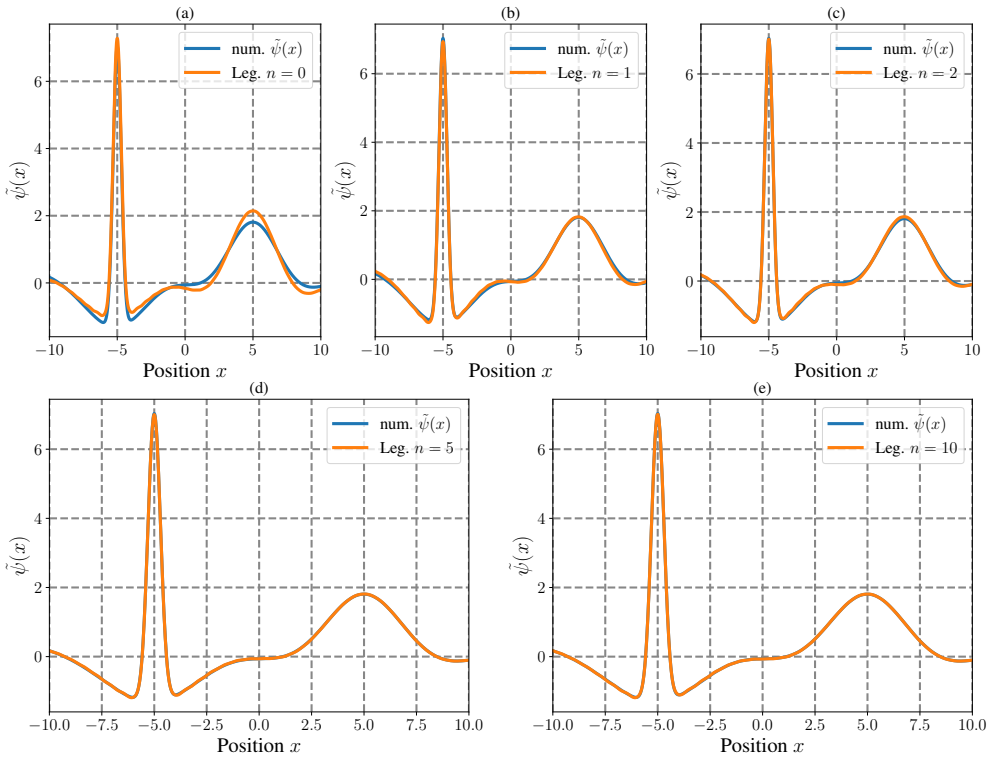

Figure 3.7: Comparison of the Legendre series expansion up to various orders with the numerical solution from fig. 3.4. **(a)** includes only the lowest order, **(b)** includes up to the 1st order, **(c)** up to the 2nd order, **(d)** up to the 5th order and **(e)** up to the 10th order. The general behavior is captured at the lowest order, with higher orders refining the approximation.

The oscillations observed in the numerical solution, as seen in fig. 3.5, are also present in the series expansion beyond the lowest order (fig. 3.9). Outside the peak intervals, the lowest order provides a better approximation than higher-order series expansions, this is apparent when comparing the original wave function $\psi(x)$ (fig. 3.1) to the lowest order reconstruction (fig. 3.9). Due to $P_0(\cos(2x_0 p/\hbar)) = 1$, the integral only consists of a sum of Gaussians with phase terms. Higher orders introduce oscillatory terms due to the cosine present in the Legendre polynomials.

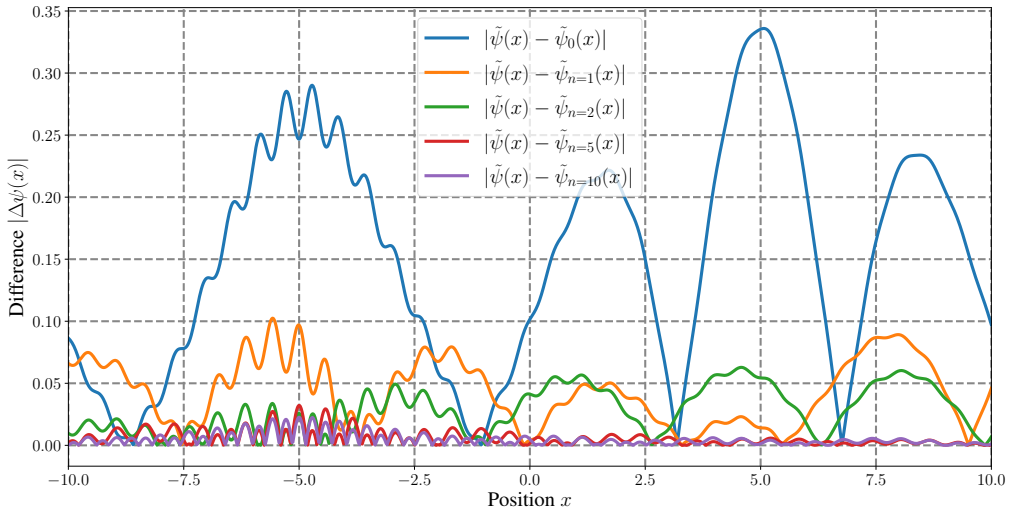

Figure 3.8: Absolute difference $|\Delta\psi(x)|$ between the series expansion $\tilde{\psi}_{\mathrm{n}}(x)$ at various orders n and the numerical solution $\tilde{\psi}(x)$ from fig. 3.4. The plot includes the lowest, 1st, 2nd, 5th, and 10th orders. Normally, one would concern themselves with the relative difference as this is what matters more. But due to the zeros of the two functions, the relative difference results in a plot that is far harder to decipher. Nonetheless, this plot can be seen in fig. A.3.

Given the relatively close approximation provided by the lowest order near the peaks and its superior performance away from the peaks, it is worth exploring the analytical reconstruction of the wave function using only the lowest order of the Legendre series. One can clearly see, that the lowest order dictates the general behavior of the function as depicted in fig. 3.10, in this figure each order is plotted individually, instead of their sum, this was done to determine which order shapes the series expansion.

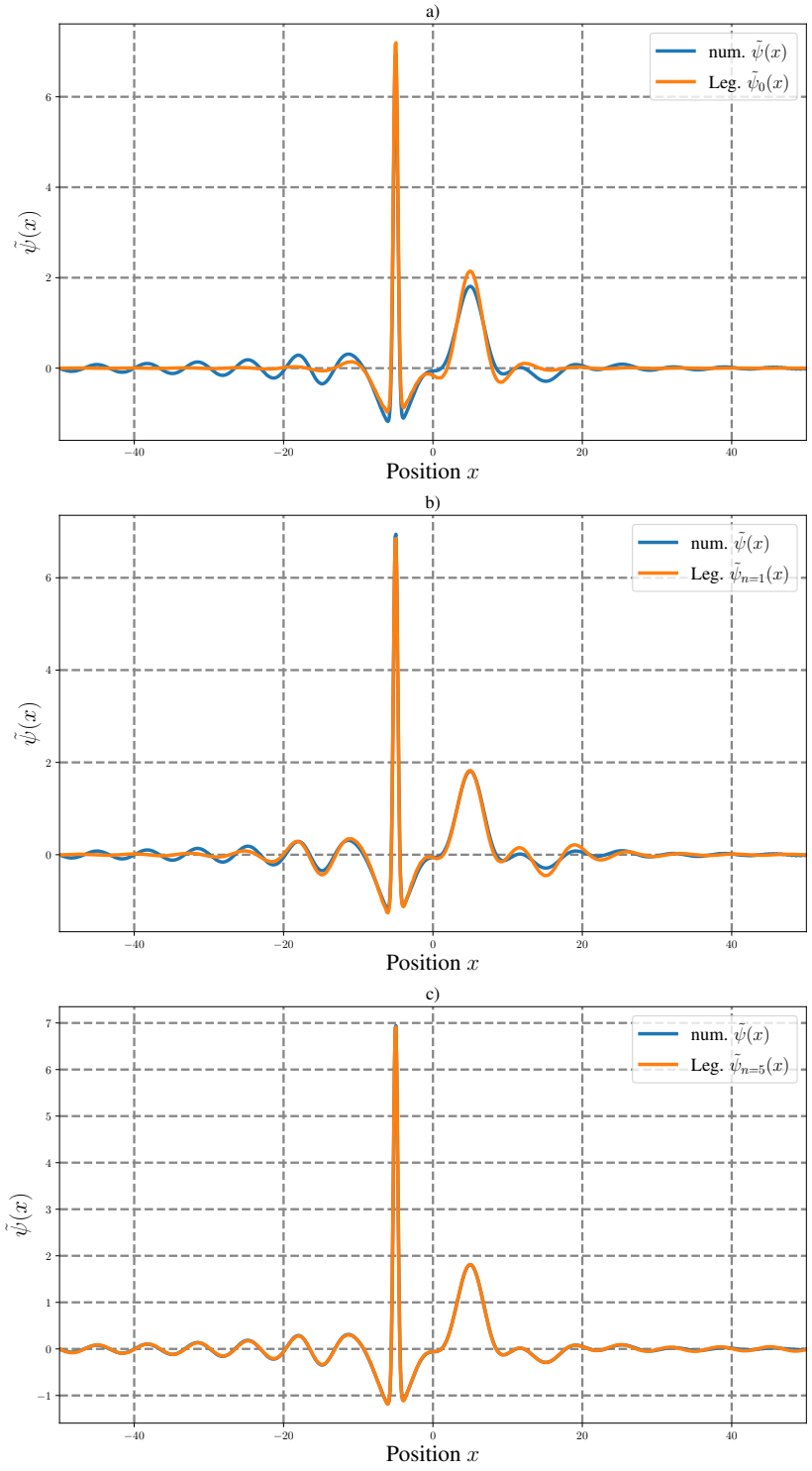

Figure 3.9: The purpose of this plot is to determine the order at which the oscillations seen in fig. 3.5 start appearing. When only looking at the lowest order no oscillations are present. At the 1st order, some oscillations appear but do not fully capture the numerical behavior. By the 5th order, the analytical and numerical results are nearly identical.

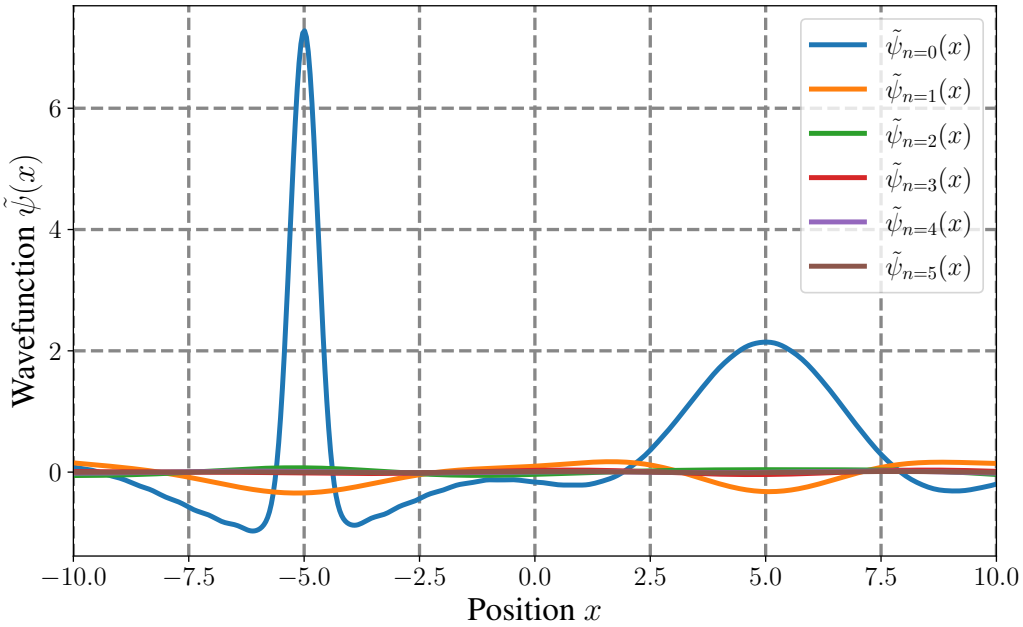

Figure 3.10: This plot shows the numerically integrated values for series expansion eq. (3.17) up to the 5th order individually. Instead of summing them, the individual orders are compared. The higher orders approach 0, as one would suspected with any series expansion.

3.3.1 Lowest order Approximation

As previously detailed the lowest order $L_0(p)$ provides a decent approximation for the reciprocal absolute value $1/|\Phi(p)|$ resulting in a simpler function, as can be seen from the definition of the Legendre Series in eq. (3.13). These factors might allow for an analytical computation. The lowest order of the series is of the form

$$L_0(p) = \begin{cases} \frac{1}{R_2}, & p < -\hbar\varepsilon \\ \frac{1}{-R_1}, & -\hbar\varepsilon < p < \hbar\varepsilon \\ \frac{1}{R_2}, & p > \hbar\varepsilon, \end{cases} \tag{3.18}$$

where once again the piecewise definition became necessary. Inserting this definition and the momentum wave function $\Phi(p)$ from eq. (3.6) into the three integrals from eq. (3.17), gives

$$\begin{aligned} I_1(x) =& \frac{1}{\sqrt{2\pi}N} \int_{-\infty}^{-\hbar\varepsilon} \mathrm{d}p\, e^{-\frac{\mathrm{i}}{\hbar}px} \left(\frac{R_1}{R_2} e^{-\frac{\mathrm{i}}{\hbar}px_0} + e^{\frac{\mathrm{i}}{\hbar}px_0} \right) = \frac{1}{\sqrt{2\pi}N}(G_1 + p_1) \\ I_2(x) =& \frac{-1}{\sqrt{2\pi}N} \int_{-\hbar\varepsilon}^{\hbar\varepsilon} \mathrm{d}p\, e^{-\frac{\mathrm{i}}{\hbar}px} \left(e^{-\frac{\mathrm{i}}{\hbar}px_0} + \frac{R_2}{R_1} e^{\frac{\mathrm{i}}{\hbar}px_0} \right) = \frac{1}{\sqrt{2\pi}N}(p_2 + G_2) \\ I_3(x) =& \frac{1}{\sqrt{2\pi}N} \int_{\hbar\varepsilon}^{\infty} \mathrm{d}p\, e^{-\frac{\mathrm{i}}{\hbar}px} \left(\frac{R_1}{R_2} e^{-\frac{\mathrm{i}}{\hbar}px_0} + e^{\frac{\mathrm{i}}{\hbar}px_0} \right) = \frac{1}{\sqrt{2\pi}N}(G_3 + p_3) \end{aligned} \tag{3.19}$$

with $\tilde{\psi}_0(x) = I_1(x) + I_1(x) + I_1(x)$. By splitting the integrals into terms only containing a phase p_k, $k \in \{1, 2, 3\}$ and terms with a Gaussian G_k, $k \in \{1, 2, 3\}$, with

$$p_k = \int_a^b \mathrm{d}p\, e^{\pm ikx_0/\hbar} \tag{3.20}$$

and

$$G_k = \int_a^b \mathrm{d}p\, \frac{R_{2,1}}{R_{1,2}}\, e^{\pm ikx_0/\hbar}, \tag{3.21}$$

where k references the integral I_k, from which the terms originate. Firstly the p_k are tackled, as these are simpler to compute. In order to solve this problem the outer terms p_1 and p_3 are combined, meaning $p_1 + p_3$, which results in

$$\int_{\hbar\varepsilon}^{\infty} \mathrm{d}p\, e^{-\mathrm{i}\frac{p}{\hbar}(x-x_0)} + \int_{-\infty}^{-\hbar\varepsilon} \mathrm{d}p\, e^{-\mathrm{i}\frac{p}{\hbar}(x-x_0)} = \int_{-\infty}^{\infty} \mathrm{d}p\, e^{-\mathrm{i}\frac{p}{\hbar}(x-x_0)} - \int_{-\hbar\varepsilon}^{\hbar\varepsilon} \mathrm{d}p\, e^{-\mathrm{i}\frac{p}{\hbar}(x-x_0)}, \tag{3.22}$$

where by moving the integration bounds, the integration could be computed analytically. This allows to integrate both of these integrals, which would not have been possible if they were to tackled individually. By using the definition for the Fourier-representation of the delta function [10],

$$\frac{1}{\sqrt{2\pi}}\int_{-\infty}^{\infty}\mathrm{d}p\; e^{-\mathrm{i}\frac{p}{\hbar}(x-x_0)} - \frac{1}{\sqrt{2\pi}}\int_{-\hbar\varepsilon}^{\hbar\varepsilon}\mathrm{d}p\; e^{-\mathrm{i}\frac{p}{\hbar}(x-x_0)} = \delta(x-x_0) - \frac{\sin(\varepsilon(x-x_0))}{\sqrt{2\pi}(x-x_0)} \tag{3.23}$$

is obtained. The remaining phase-term is p_2 is similar to the second term of eq. (3.23), thus it can be integrated in the same way, this yields

$$-\frac{1}{\sqrt{2\pi}}\int_{-\hbar\varepsilon}^{\hbar\varepsilon}\mathrm{d}p\; e^{-\mathrm{i}\frac{p}{\hbar}(x+x_0)} = -\frac{\sin(\varepsilon(x+x_0))}{\sqrt{2\pi}(x+x_0)}. \tag{3.24}$$

With the p_k now computed, the focus shifts to the G_k terms. Once again G_1 and G_3 are computed together. By starting with a similar rewrite as used in eq. (3.22), the bounds are changed to

$$\begin{aligned} G_1 + G_3 &= \int_{\hbar\varepsilon}^{\infty}\mathrm{d}p\; e^{-\mathrm{i}\frac{p}{\hbar}(x+x_0)}\frac{R_1}{R_2} + \int_{-\infty}^{-\hbar\varepsilon}\mathrm{d}p\; e^{-\mathrm{i}\frac{p}{\hbar}(x-x_0)}\frac{R_1}{R_2} \\ &= \int_{-\infty}^{\infty}\mathrm{d}p\; e^{-\mathrm{i}\frac{p}{\hbar}(x-x_0)}\frac{R_1}{R_2} - \int_{-\hbar\varepsilon}^{\hbar\varepsilon}\mathrm{d}p\; e^{-\mathrm{i}\frac{p}{\hbar}(x-x_0)}\frac{R_1}{R_2}, \end{aligned} \tag{3.25}$$

thus enabling us to solve the first integral, while the second remains analytically unsolvable. The first of these two integrals, can be integrated using the Gaussian integral,

$$\int_{-\infty}^{\infty}\mathrm{d}p\; e^{-\mathrm{i}\frac{p}{\hbar}(x-x_0)}\frac{R_1}{R_2} = \sqrt{\frac{\sigma_1}{\sigma_2}}\frac{1}{\sqrt{\sigma_1^2-\sigma_2^2}}e^{-\frac{1}{2}\frac{(x-x_0)^2}{\sigma_1^2-\sigma_2^2}}. \tag{3.26}$$

This is the last term that can be calculated analytically as the remaining integrals, the second term form eq. (3.25) and G_2, can not be integrated analytically. This due to the fact, that they are Gaussian integrals with finite bounds. By combing the remaining integral from eq. (3.25) with G_2, we obtain

$$\frac{1}{\sqrt{2\pi}N}\int_{-\hbar\varepsilon}^{\hbar\varepsilon}\mathrm{d}p\left(e^{-\mathrm{i}\frac{p}{\hbar}(x-x_0)}\frac{R_1}{R_2} + e^{-\mathrm{i}\frac{p}{\hbar}(x+x_0)}\frac{R_2}{R_1}\right). \tag{3.27}$$

Therefore the whole reconstructed function is

$$\begin{aligned}\tilde{\psi}_0(x) =& \frac{1}{N}\Bigg[\delta(x-x_0) - \frac{\sin(\varepsilon(x+x_0))}{\sqrt{2\pi}(x+x_0)} + \sqrt{\frac{\sigma_1}{\sigma_2}}\frac{1}{\sqrt{\sigma_1^2-\sigma_2^2}} e^{-\frac{1}{2}\frac{(x-x_0)^2}{\sigma_1^2-\sigma_2^2}} \\ & - \frac{\sin(\varepsilon(x-x_0))}{\sqrt{2\pi}(x-x_0)} - \frac{1}{\sqrt{2\pi}}\int_{-\hbar\varepsilon}^{\hbar\varepsilon} \mathrm{d}p \left(e^{-\mathrm{i}\frac{p}{\hbar}(x-x_0)}\frac{R_1}{R_2} + e^{-\mathrm{i}\frac{p}{\hbar}(x+x_0)}\frac{R_2}{R_1}\right)\Bigg].\end{aligned} \tag{3.28}$$

Unfortunately, the lowest order approximation can not be entirely computed analytically.

While the lowest order provides a reasonably good approximation for the reconstructive function, its general applicability remains questionable. This is primarily due to the inability to compute it analytically and the relatively small computational cost difference between the lowest order and higher-order terms. As a result, the lowest order approximation does not offer significant advantages in practice. Consequently, this approach did not lead to an analytic solution. A comparison between the original function $\psi(x)$, the direct numerical reconstruction $\tilde{\psi}(x)$ and the lowest order reconstruction $\tilde{\psi}_0(x)$ is depicted in fig. 3.11.

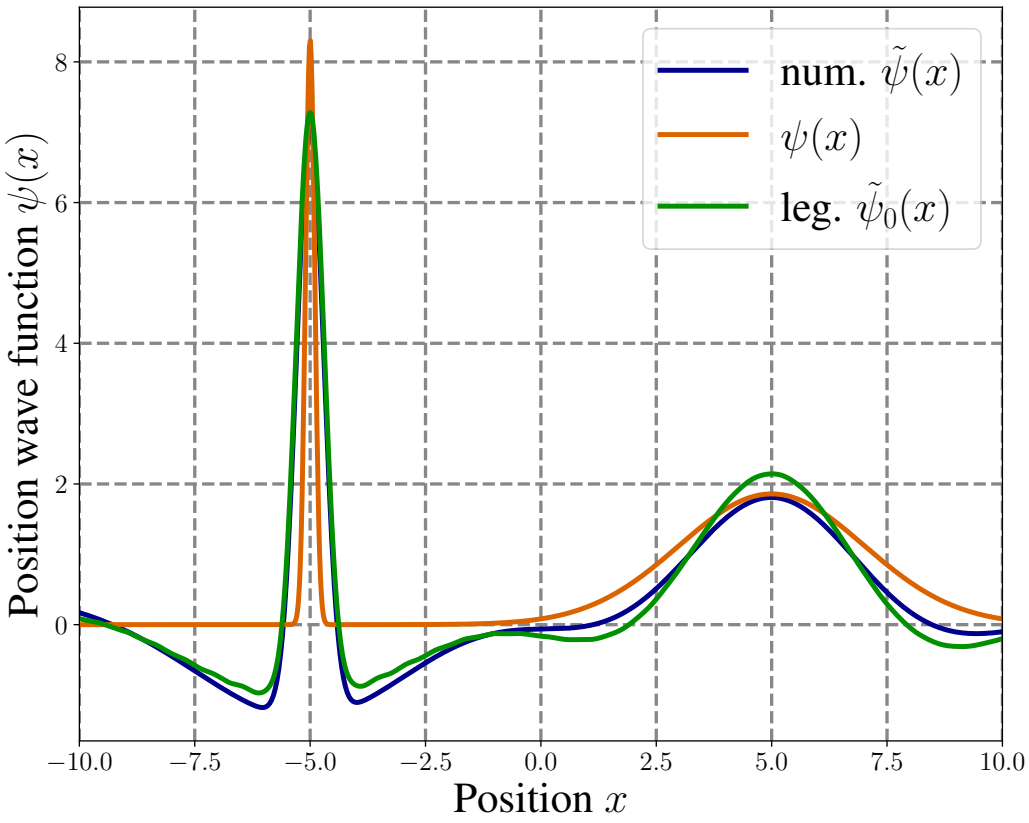

Figure 3.11: The plot depicts a comparison of the lowest order reconstruction $\tilde{\psi}_0(x)$, to the direct numerical reconstruction $\tilde{\psi}(x)$ and a scaled version of the original $\psi(x)$, from eq. (3.1), which was scaled by the mean value of the quotient of the peaks. The lowest order of the series expansion is once again similar to the numerical reconstruction, which it approximates.

4 Discussion and Conclusion

The results of this thesis emphasize the important role of the phase in the momentum wave function, demonstrating its ability to encode essential information about the original position wave function, by reconstructing a exemplary wave function, consisting of a super position of two Gaussians. This work builds on insights by Oppenheim and Lim [3], who originally explored the importance of phase in signal processing, by applying their methodology analytically. Through demonstrating the applicability of their principles in quantum mechanics, this thesis illustrates that methods from classical signal processing could provide new insights in quantum mechanics.

One of the main findings of this work is the reconstruction of position wave functions using phase-only information derived from the momentum wave function. By adapting the protocol, first used by Oppenheim and Lim, to the quantum mechanical framework, this thesis demonstrates that the phase of the momentum wave function is enough to retrieve significant aspects of the position wave function. In this specific example, it was possible to restore the essential components, for example the expectation values, of a position wave function composed of two Gaussians.

However it is important to mention, that this thesis is no general proof, but rather a demonstration of the validity for a specific example. With the chosen exemplary wave function, it was possible to reconstruct the wave function closely to the original. But by applying the protocol onto a single Gaussian, it becomes apparent, that in this example only the position can be regained, while the variance is lost, which is depicted in appendix A.1.

This leads to the conclusion that the protocol, when applied to a super position of two Gaussians, does not reconstruct the variance but rather some relative factor, made up by the two variances, which keeps the behavior similar to the original. The impact of this difference might be small, as it seems that despite it the reconstruction still provides a good approximation for the original wave function. In signal processing the phase of the transformed image is known to contain the information about the spatial arrangement, the edges and silhouettes present with in an image [4, 11]. This might be the reason, while in the example the position of the peaks is retained exactly, while the variances might only be preserved relative to one another. This might also explain, why the width of the single Gaussian is discarded entirely.

Furthermore, the use of the Legendre series expansion as an approximation method revealed that even the lowest order approximation provides a reasonable representation of the wave function. However, higher-order terms introduce oscillatory corrections that

improve the approximation. But higher-order calculations also increase the complexity of the reconstruction process. Due to this, an approximation via a Legendre series does not seem sensible. This conclusion was reached because the necessary piecewise definition makes the resulting integrals difficult to calculate, and the numerical computation time increases significantly with higher orders. As a result, this approach offers no practical advantage, when compared to the direct numerical reconstruction.

The ability to reconstruct position wave functions using only phase information has potential applications in quantum information science, where phase plays a pivotal role in encoding and processing information. Moreover, methods developed based on this work could inform experimental techniques for wave function analysis. The protocol discussed in section 2.2 could enable the determination of the position wave function using only momentum phase measurements. Since the phase is momentum-dependent, it may be measurable through interference techniques [12], allowing the position wave function to be computed from this information. But through interference experiments only relative phases are measurable, which may be a limiting factor.

There are also more limits to the reconstruction based on the protocol. The numerical solution exhibited oscillations, likely arising form the limited nature of phase based reconstruction [13]. In thus instance, the reconstructed wave function showed oscillations, particularly in regions without significant peaks. This highlights the need for further refinement of the reconstruction protocol.

If this work were to be expanded upon, there are several avenues for future research. First, refining the reconstruction protocol to mitigate numerical noise and interference effects would enhance the reliability of phase-only reconstructions. In the realm of signal processing these reconstructions have gotten more precise, as the methods improved [14]. Second, exploring alternative basis functions or series expansions could provide more efficient approximations with fewer computational demands. Third, applying these methods to more complex wave functions with strongly interfering components would test their generality and robustness. At last it also might be interesting to declare a metric in order to quantify the similarities or differences between the original wave function and its reconstruction.

Bibliography

[1] M. Born, "Zur quantenmechanik der stossvorgaenge", Zeitschrift fuer Physik **37**, 863–867 (1926) 10.1007/bf01397477.

[2] D. J. Griffiths, ***Introduction to quantum mechanics*** (Prentice Hall, Englewood Cliffs, NJ [u.a.], 1995).

[3] A. Oppenheim and J. Lim, "The importance of phase in signals", Proceedings of the IEEE **69**, 529–541 (1981) 10.1109/proc.1981.12022.

[4] M. Hayes, J. Lim, and A. Oppenheim, "Phase-only signal reconstruction", in Icassp '80. ieee international conference on acoustics, speech, and signal processing, Vol. 5 (1980), pages 437–440, 10.1109/icassp.1980.1171031.

[5] R. Gonzalez and R. Woods, ***Digital Image Processing Global Edition*** (Pearson Deutschland, 2017), page 1024.

[6] J. Walker, ***Fast fourier transforms, second edition***, Studies in Advanced Mathematics (Taylor & Francis, 1996).

[7] L. Cohen, ***Time-frequency analysis***, Electrical engineering signal processing (Prentice Hall PTR, 1995).

[8] P. Virtanen, Gommers, and S. 1. 0. Contributors, "Scipy 1.0–fundamental algorithms for scientific computing in python", Nature Methods 17, 261 (2020) **17**, 261–272 (2019) 10.1038/s41592-019-0686-2, arXiv:1907.10121 [cs.MS].

[9] G. B. Arfken, H.-J. Weber, and F. E. Harris, editors, ***Mathematical methods for physicists***, 7. ed., Previous ed.: Amsterdam; London: Elsevier Academic, 2005. - Includes bibliographical references and index. - Description based on print version record (Academic, Oxford, 2013), 1 page.

[10] D. Mitrović and D. Žubrinić, ***Fundamentals of applied functional analysis, Distributions - sobolev spaces - nonlinear elliptic equations***, 1. publ., Pitman monographs and surveys in pure and applied mathematics 91, Bibliography: p388-393. - Includes index (Longman, Harlow, 1998), 399 pages.

[11] Y. Shapiro and M. Porat, "Image representation and reconstruction from spectral amplitude or phase", in 1998 ieee international conference on electronics, circuits and systems. surfing the waves of science and technology (cat. no.98ex196), Vol. 2, ICECS-98 (1980), pages 461–464, 10.1109/icecs.1998.814921.

[12] I. P. Ivanov, D. Seipt, A. Surzhykov, and S. Fritzsche, "Double-slit experiment in momentum space", EPL 115 (2016) no.4, 41001 **115**, 41001 (2016) 10.1209/0295-5075/115/41001, arXiv:1606.04732 [quant-ph].

[13] M. H. Hayes, "The reconstruction of a multidimensional sequence from the phase or magnitude of its fourier transform", IEEE Transactions on Acoustics, Speech, and Signal Processing **30**, 140–154 (1982).

[14] D. Lopes and P. White, "Signal reconstruction from the magnitude or phase of a generalised wavelet transform", **2015** (2000).

[15] E. Wigner, "On the quantum correction for thermodynamic equilibrium", Physical Review **40**, 749–759 (1932) 10.1103/physrev.40.749.

[16] E. Colomés, Z. Zhan, and X. Oriols, "Comparing wigner, husimi and bohmian distributions: which one is a true probability distribution in phase space?", Journal of Computational Electronics **14**, 894–906 (2015) 10.1007/s10825-015-0737-6.

[17] M. Hillery, R. O'Connell, M. Scully, and E. Wigner, "Distribution functions in physics: fundamentals", Physics Reports **106**, 121–167 (1984) 10.1016/0370-1573(84)90160-1.

[18] M. Nielsen and I. Chuang, ***Quantum computation and quantum information: 10th anniversary edition*** (Cambridge University Press, 2010).

A Appendix

A.1 The protocol applied to a single Gaussian

The point of this section is to show that for a simple wave function some of the structural information gets lost. To demonstrate the protocol is applied onto a wave function composed of a single Gaussian.
To start, the wave function $\psi_1(x)$ is established as

$$\psi_1(x) = \frac{1}{\sqrt[4]{\pi\sigma^2}} e^{-\frac{1}{2}\frac{x^2}{\sigma^2}}, \tag{A.1}$$

which has the two characteristics an expectation value of $x_0 = 0$ and a width σ. The Fourier transform for a Gaussian has already been calculated in the main part. Therefore the momentum wave function is:

$$\Phi_1(p) = \sqrt[4]{\frac{\sigma^2}{\pi}} e^{-\frac{1}{2\hbar^2}p^2\sigma^2}. \tag{A.2}$$

Due to the fact, that the wave function is completely real, that is $|\Phi_1(p)| = \Phi_1(p)$, for any position wave centered around another point, the phase is only determined by the shift in eq. (3.5). Thus the reconstruction integral is

$$\tilde{\psi}_1(x) = \frac{1}{\sqrt{2\pi}} \int_{-\infty}^{\infty} \mathrm{d}p\, e^{-\frac{\mathrm{i}}{\hbar}px} \frac{\Phi_1(p)}{|\Phi_1(p)|} = \frac{1}{\sqrt{2\pi}} \int_{-\infty}^{\infty} \mathrm{d}p\, e^{-\frac{\mathrm{i}}{\hbar}px}. \tag{A.3}$$

This integral is the definition of the delta function [10], which results in

$$\tilde{\psi}_1(x) = \delta(x). \tag{A.4}$$

It becomes apparent, that the position of the maximum was preserved, while the width was not. Which leads to the suspicion, that the protocol does not preserve the width but rather a relative width determined by a combination of the two variances present within the main example, given by eq. (3.1).

A.2 The Wigner Function of the exemplary Wave Function

In order to further our understanding of the behavior of the example wave function $\psi(x)$, given by eq. (3.1), its Wigner function was analyzed. The Wigner function allows insight to both momentum and position space [15], providing an overview of both position and momentum variables. Importantly, the probability distributions for each variable can be obtained by integrating over the other [16]. Additionally, as a Fourier-based transformation, the Wigner function closely aligns with the principles of the protocol, defined in section 2.2, which is applied to the wave function [17].

The goal is to calculate the Wigner function of the example wave function to gain deeper insights into its phase space characteristics.

Once again, the starting point is the general form provided in eq. (3.1). By plugging the wave function $\psi(x)$ into the definition for the Wigner function [15],

$$W(x,p) = \frac{1}{\pi\hbar} \int_{-\infty}^{\infty} \mathrm{d}y \; e^{\frac{\mathrm{i}}{\hbar}py} \; \psi^*\left(x + \frac{y}{2}\right)\psi\left(x - \frac{y}{2}\right). \tag{A.5}$$

Due to the original wave function being completely real, the complex conjugation becomes irrelevant as $\psi^* = \psi$. Thus inserting the wave function,

$$W(x,p) = \frac{1}{\pi\hbar N^2} \int_{-\infty}^{\infty} \mathrm{d}y \; e^{\frac{\mathrm{i}}{\hbar}py} \left[\psi_1\left(x+\frac{y}{2}\right)+\psi_2\left(x+\frac{y}{2}\right)\right]\left[\psi_1\left(x-\frac{y}{2}\right)+\psi_2\left(x-\frac{y}{2}\right)\right], \tag{A.6}$$

provides the Wigner function. In order to simplify calculations the previously defined $\psi_{\mathrm{n}}(x) = \frac{1}{\sqrt[4]{\pi\sigma_{\mathrm{n}}^2}} e^{-\frac{1}{2}\frac{x^2}{\sigma_{\mathrm{n}}^2}}$ is used. By now calculating the brackets, a pattern emerges, with

$$W(x,p) = \frac{1}{\pi\hbar N^2} \int_{-\infty}^{\infty} \mathrm{d}y \; e^{\frac{\mathrm{i}}{\hbar}py} \left[\psi_1^+\psi_1^- + \psi_1^+\psi_2^- + \psi_2^+\psi_1^- + \psi_2^+\psi_1^-\right]. \tag{A.7}$$

Here $\psi_{\mathrm{n}}^{\pm} = \psi_{\mathrm{n}}(x \pm \frac{y}{2})$ is introduced, as each of the remaining four terms within the Wigner function is a cross of ψ_{j}^+ and ψ_{k}^-. Therefore the Wigner function can be separated into four integrals.

These Integrals are

$$W_{\mathrm{k,j}}(x,p) = \frac{1}{\pi\hbar N^2} \int_{-\infty}^{\infty} \mathrm{d}y \; e^{\frac{\mathrm{i}}{\hbar}py} \psi_k^+\psi_j^- \tag{A.8}$$

with $k,\ j \in \{1,\ 2\}$. The two cross terms ($k \neq j$) and the two non cross terms ($k = j$) are similar to calculate, thus reducing the it to only two integrations, in order to obtain the desired results. The first term of concern is the first non cross term $W_{1,1}(x,p)$.

Proceeding by plugging in $\psi_1(x)$ and rearranging, results in

$$W_{1,1}(x,p) = \frac{1}{\pi\hbar N^2}\frac{1}{\sqrt{\pi}\sigma_1}\int_{-\infty}^{\infty} \mathrm{d}y\; e^{\frac{\mathrm{i}}{\hbar}py}\; e^{-\frac{y^2}{4\sigma_1^2}} e^{-\frac{1}{2\sigma_1^2}(x-x_0)^2}. \tag{A.9}$$

This integral can be solved by using the formula for Gaussian integrals and results in [2]

$$W_{1,1}(x,p) = \frac{2}{\pi\hbar N^2} e^{-\frac{\sigma_1^2}{\hbar^2}p^2}\; e^{-\frac{1}{2\sigma_1^2}(x-x_0)^2}. \tag{A.10}$$

The second non cross term $W_{2,2}(x,p)$ is equivalent, as it is only an exchange of indices. The integral is

$$W_{2,2}(x,p) = \frac{1}{\pi\hbar N^2}\frac{1}{\sqrt{\pi}\sigma_2}\int_{-\infty}^{\infty} \mathrm{d}y\; e^{\frac{\mathrm{i}}{\hbar}py}\; e^{-\frac{y^2}{4\sigma_2^2}} e^{-\frac{1}{2\sigma_2^2}(x+x_0)^2} \tag{A.11}$$

which similar to eq. (A.10) and therefore results in

$$W_{2,2}(x,p) = \frac{2}{\pi\hbar N^2} e^{-\frac{\sigma_2^2}{\hbar^2}p^2}\; e^{-\frac{1}{2\sigma_2^2}(x+x_0)^2}. \tag{A.12}$$

With these terms settled, the focus is shifted to the cross terms. These two are very similar to each other with $W_{1,2}(x,p)$ being

$$W_{1,2}(x,p) = \frac{1}{\pi\hbar N^2}\frac{1}{\sqrt{\pi\sigma_1\sigma_2}}\int_{-\infty}^{\infty} \mathrm{d}y\; e^{\frac{\mathrm{i}}{\hbar}py}\; e^{-\frac{y^2}{8}a}\; e^{-\frac{1}{2}y(bx+ax_0)}\; e^{\theta(x)} \tag{A.13}$$

with $a = \frac{1}{\sigma_1^2} + \frac{1}{\sigma_2^2}$, $b = \frac{1}{\sigma_1^2} - \frac{1}{\sigma_2^2}$ and $\theta(x) = -\frac{a}{2}x^2 - \frac{a}{2}x_0 + bxx_0$. This can once again be integrated by using the Gaussian integral resulting in [2]

$$W_{1,2}(x,p) = \frac{1}{\pi\hbar N^2}\frac{1}{\sqrt{\sigma_1\sigma_2}}\sqrt{\frac{8}{a}}\; e^{-\frac{2}{a\hbar^2}p^2}\; e^{-\frac{1}{2}x^2\frac{a^2+b^2}{a}}\; e^{-\frac{2i}{a\hbar}p(bx+ax_0)}. \tag{A.14}$$

The other cross term $W_{2,1}(x,p)$ can be done similarly and only differs in one sign,

$$W_{2,1}(x,p) = \frac{1}{\pi\hbar N^2}\frac{1}{\sqrt{\sigma_1\sigma_2}}\sqrt{\frac{8}{a}}\; e^{-\frac{2}{a\hbar^2}p^2}\; e^{-\frac{1}{2}x^2\frac{a^2+b^2}{a}}\; e^{+\frac{2i}{a\hbar}p(bx+ax_0)}. \tag{A.15}$$

The two cross terms combine to make up the interference term, $W_{\mathrm{int}}(x,p) = W_{1,2}(x,p) + W_{2,1}(x,p)$ where the sign difference results in a cosine function,

$$W_{\mathrm{int}} = \frac{1}{\pi\hbar N^2}\frac{2}{\sqrt{\sigma_1\sigma_2}}\sqrt{\frac{8}{a}}\; e^{-\frac{2}{a\hbar^2}p^2}\; e^{-\frac{1}{2}x^2\frac{a^2+b^2}{a}}\; \cos\!\left(-\frac{2}{a\hbar}p(bx+ax_0)\right). \tag{A.16}$$

By recombining the three terms, the full Wigner function for the original wave function $\psi(x)$ is obtained, which is

$$W(x,p) = \frac{2}{\pi\hbar N^2}\Bigg[e^{-\frac{\sigma_1^2}{\hbar^2}p^2}\; e^{-\frac{1}{2\sigma_1^2}(x+x_0)^2} + e^{-\frac{\sigma_2^2}{\hbar^2}p^2}\; e^{-\frac{1}{2\sigma_2^2}(x+x_0)^2} + \frac{2}{\sqrt{\sigma_1\sigma_2}}\sqrt{\frac{8}{a}}\; e^{-\frac{2}{a\hbar^2}p^2}\; e^{-\frac{1}{2}x^2\frac{a^2+b^2}{a}}\; \cos\left(-\frac{2}{a\hbar}p(bx+ax_0)\right)\Bigg]. \tag{A.17}$$

Two regular Wigner functions corresponding to the individual Gaussian components of the wave function can be distinguished in eq. (A.17). Additionally to the two Gaussian parts, the interference term introduces oscillatory patterns between the in between the two peaks. These interference effects highlight the quantum coherence in the system. Similarly, such interference would be observed by calculating the absolute square of the original wave function $\psi(x)$ in position space, but the Wigner function provides a richer, phase-space perspective.

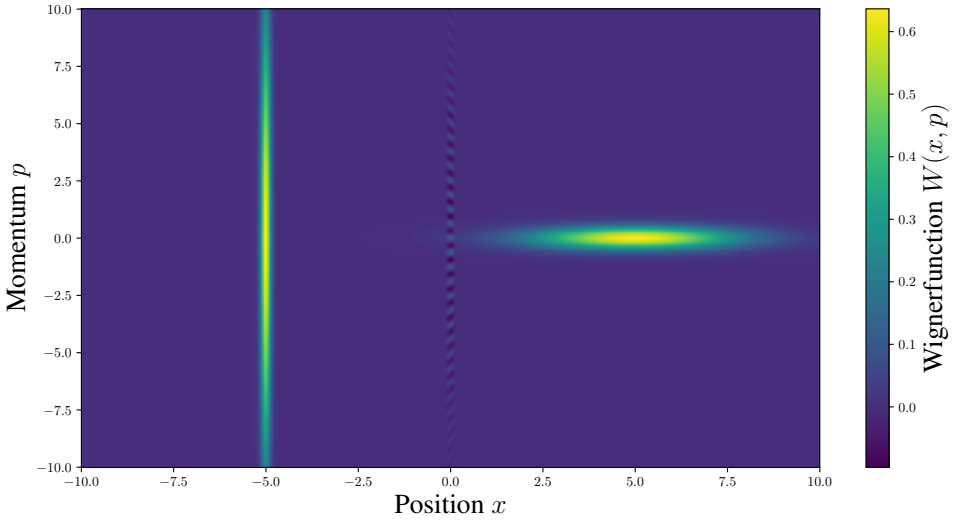

Figure A.1: Plot of eq. (A.17). The two Gaussian-like peaks appear as 2D-Gaussians in phase space, corresponding to the two components of the wave function. Between these peaks, a hint of the interference pattern generated by eq. (A.16) is observed. The values used are $x_0 = 5$, $\sigma_1 = 2$, and $\sigma_2 = 0.1$. This plot utilized $\hbar = 1$, as it provides better visibility.

The Wigner function, as seen in fig. A.1, can be easily utilized to find the individual behavior of the wave function in position and momentum space, as it is determined by focusing on either axis. The behavior along these axes corresponds directly to the position wave function $\psi(x)$ in eq. (3.1) and the momentum-space representation of the wave function $\Phi(x)$ shown in fig. 3.2. This reinforces the utility of the Wigner function in bridging the two domains and providing a comprehensive phase-space representation

of the quantum state.

A.2.1 The Interference term

While deriving the Wigner function for the original wave function composed of two Gaussians, the interference term

$$W_{\text{int}} = \frac{1}{\pi\hbar N^2}\frac{2}{\sqrt{\sigma_1\sigma_2}}\sqrt{\frac{8}{a}}\ \phi_{\text{p}}(p)\psi_{\text{x}}(x)\ \cos\left(-\frac{2}{a\hbar}p(bx+ax_0)\right) \tag{A.18}$$

appeared, with $\phi_{\text{p}}(p) = e^{-\frac{2}{a\hbar^2}p^2}$ and $\psi_{\text{x}}(x) = e^{-\frac{1}{2}x^2\frac{a^2+b^2}{a}}$ being two Gaussians, with each only dependent on one of the two variables x and p. But the most interesting part of the function is the cosine term, as due to its form, hyperbolic phase lines are created. The hyperbolic phase lines arise because the argument of the cosine function is proportional to the reciprocal of $(bx + ax_0)$. Setting the argument to a constant c and rearranging gives

$$p = -\frac{a\hbar c}{2(bx+ax_0)}. \tag{A.19}$$

This equation describes a family of hyperbolic curves in phase space. These phase lines are not as easily visible in fig. A.1, as the whole interference term approaches zero rather quickly due to the exponential decay and small overlap of the Gaussians present within the term. In order to show this rather interesting behavior, only the cosine parts of the function were plotted, by setting everything else, including the Gaussians, pre-factors and the constants, equal to one. This results in

$$Q(x,p) \equiv \cos\left(-\frac{2}{a}p(bx+ax_0)\right). \tag{A.20}$$

A plot of this function is shown in fig. A.2.

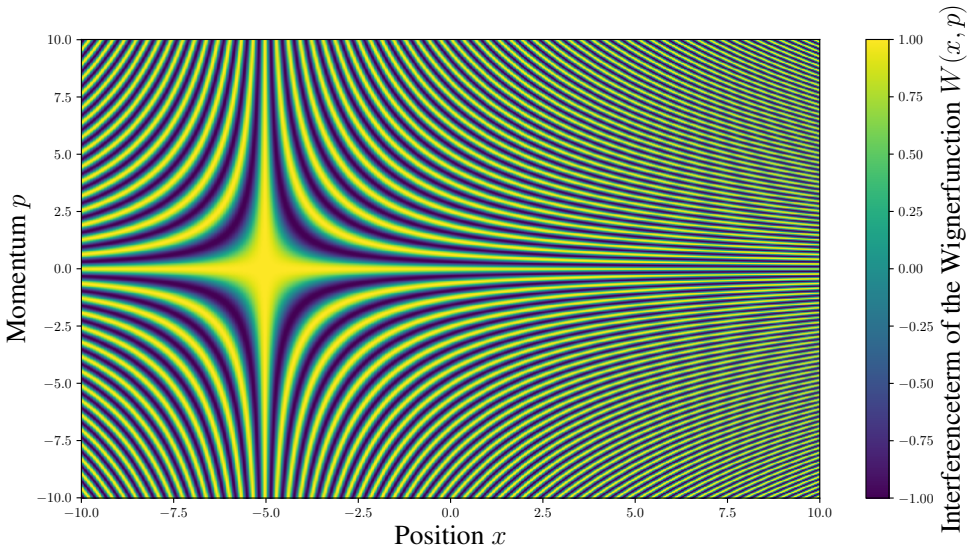

Figure A.2: Plot of eq. (A.20), done to demonstrate the hyperbolic behavior of the phase lines, due to the cosine being a symmetric function, it is symmetric around $p = 0$ and $x = -x_0$, as this point is extrema of the hyperbolic function. This combination of the hyperbolic structure and the oscillatory nature of the cosine function creates the characteristic interference pattern. The values used are $x_0 = 5$, $\sigma_1 = 2$, and $\sigma_2 = 0.1$.

A.3 Relative Difference between the Legendre and Numerical Reconstruction

As discussed in section 3.3 the Legendre series expansion provides a good approximation for the reciprocal absolute value $1/|\Phi(p)|$ of the momentum wave function. In order to demonstrate this, the difference between the numerical integration over the absolute value (fig. 3.4) and over different orders of the Legendre Series (fig. 3.7) is shown. The difference, which was analyzed in fig. 3.8, is the absolute difference, but for completeness sake the relative difference is also included. This is the go to when analyzing approximations in relation to the original, but due to the zeros present within both the approximation and the original,the plot is rather hard to decipher. Nonetheless the relative difference as can be seen in fig. A.3.

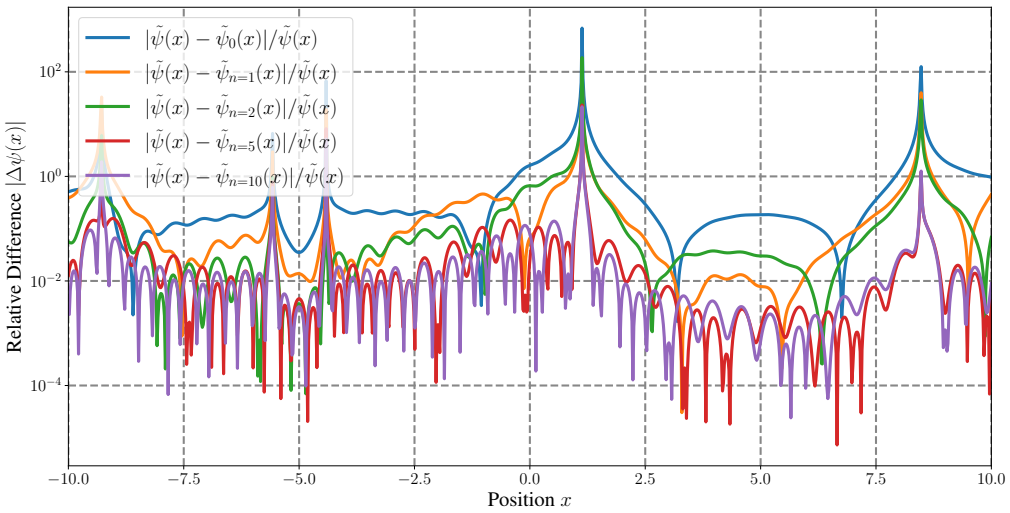

Figure A.3: The relative difference between the numerical reconstruction $\tilde{\psi}(x)$ (fig. 3.4) and various series expansions up to different orders is shown. This plot is excluded from the main thesis because the zeros of the numerical solution make it difficult to clearly observe the desired behavior, as it provides only limited insights into the convergence of the series expansion. The parameters used are $x_0 = 5$, $\sigma_1 = 2$, and $\sigma_2 = 0.1$.